Synthesis of Covalent Organic Framework and it's Potential Applications

M.Sc. Thesis

By

SUPRATIM GHOSH

DEPARTMENT OF CHEMISTRY

INDIAN INSTITUTE OF TECHNOLOGY INDORE

May, 2024

Synthesis of Covalent Organic Framework and it's Potential Applications

A THESIS

Submitted in partial fulfillment of the requirements for the award of the degree

of

Master of Science

by

SUPRATIM GHOSH

DEPARTMENT OF CHEMISTRY

INDIAN INSTITUTE OF TECHNOLOGY INDORE

May, 2024

INDIAN INSTITUTE OF TECHNOLOGY INDORE

CANDIDATE'S DECLARATION

I hereby certify that the work which is being presented in the thesis entitled **"Synthesis of Covalent Organic Framework and it's Potential Applications"** in the partial fulfillment of the requirements for the award of the degree of **Master of Science** and submitted to the **Department of Chemistry**, **Indian Institute of Technology Indore**, is an authentic record of my own work carried out from 15th July, 2023 to 6th May, 2024 under the supervision of **Prof. Apurba K. Das**, Professor, Department of Chemistry, Indian Institute of Technology Indore,

The matter presented in this thesis has not been submitted by me for the award of any other degree of this or any other institute.

Supratim Ghosh

06/05/2024

Supratim Ghosh

This is to certify that the above statement made by the candidate is correct to the best of my knowledge.

6/5/2024

Prof. Apurba K. Das

SUPRATIM GHOSH has successfully given his M.Sc. Oral Examination held on May 10, 2024.

6/5/2024

Signature of Supervisor of M.Sc. Thesis	Convener, DPGC
Prof. Apurba K. Das	**Dr. Umesh A. Kshirsagar**
Date: 06/05/2024	Date:

ACKNOWLEDGEMENTS

I would like to express my special thanks of gratitude to Prof. Apurba K. Das for his constant support, guidance, cooperation and encouragement. I am fortunate enough to have the opportunity of working under his guidance and was able to accumulate valuable experience and have learned some aspects of Organic Chemistry.

I would also like to extend my gratitude to my PSPC members Dr. Tridib Kumar Sarma and Dr. Pravarthana Dhanapal, for their sincere recommendation and motivation. I thank Prof. Tushar Kanti Mukherjee, Head of Department, Chemistry and DPGC Convenor, Dr. Umesh A. Kshirsagar for their suggestions and assistance.

I also want to express my gratitude to Prof. Suhas Joshi, Director, IIT Indore for providing the resources and a stimulating research environment. I would also take this opportunity to thank SIC, IIT Indore and Chemistry Office for their assistance and technical support, without which it would not have been possible to work on this project.

I would also like to thank my lab mates for their constant encouragement and support.

I also acknowledge with a deep sense of reverence towards my parents and my family members, who have always supported me morally and mentally and have encouraged me constantly. It is the kindness of these acknowledged persons that I have been able to make progress in this project successfully. Without their guidance I would not have made any headway in this research project.

SUPPRATIM GHOSH

Department of Chemistry, IIT Indore

Dedicated to my family

ABSTRACT

In this project, our target is to synthesize a pristine, stable bis-benzothiazole linked covalent organic framework (COF) via a one pot synthesis. Out of the two monomers required, 2,5-diamino-1,4-benzenedithiol dihydrochloride (DABT) is available commercially. The other monomer, [1,1':4',1"-terphenyl]-3,3",5,5"-tetracarbaldehyde (TPTC) is synthesized by employing Suzuki-Miyaura cross-coupling reaction. The synthesized compound is characterized using ^{1}H and ^{13}C NMR spectroscopy. The COP is synthesized further by varying the reaction conditions and characterized by FT-IR, PXRD, FE-SEM, TGA and BET analysis. The chemical stability of our synthesized TBBTCOP was checked in different solvents. Further we also performed a post-synthetic modification on our COP by incorporating copper into it and utilized it for Chan-Lam coupling reaction between various substrates.

TABLE OF CONTENTS

LIST OF FIGURES

LIST OF SCHEMES

NOMENCLATURE

δ	Chemical shift
°C	Degree Centigrade
g	gram
µL	microlitres
mg	milligrams
mL	millilitres
mmol	millimoles
nm	nanometre
ppm	parts per million

ACRONYMS

BET	Brunauer-Emmett-Teller
DCM	Dichloromethane
DMF	*N*,*N*-Dimethylformamide
EtOAc	Ethyl acetate
FE-SEM	Field Emission Scanning Electron Microscope
FT-IR	Fourier Transform Infrared
HCl	Hydrogen chloride
H_2SO_4	Sulfuric acid
KOAc	Potassium acetate
K_2CO_3	Potassium carbonate
K_3PO_4	Potassium phosphate
MnO_2	Manganese dioxide
MeOH	Methanol
Na_2CO_3	Sodium carbonate
Na_2SO_4	Sodium sulfate
NMP	*N*-methyl-2-pyrrolidone
NMR	Nuclear Magnetic Resonance
$Pd(PPh_3)_4$	Tetrakis(triphenylphosphine)-palladium(0)
$Pd(dppf)Cl_2$	[1,1′-Bis(diphenylphosphino) ferrocene]dichloropalladium(II)
SeO_2	Selenium dioxide
TGA	Thermogravimetric analysis
THF	Tetrahydrofuran

Chapter 1

INTRODUCTION

Since the first development of covalent organic frameworks (COFs) in 2005 by Yaghi and his co-workers[1], there has been a significant growth in this field. Belonging to the class of porous materials, COFs have been synthesized from simple atoms like carbon, nitrogen, oxygen and sulphur using previously known and simple organic reactions like Schiff base condensation, boronic ester condensation, C-C coupling reactions and many more leading to extensive 2D and 3D network structures of low density.

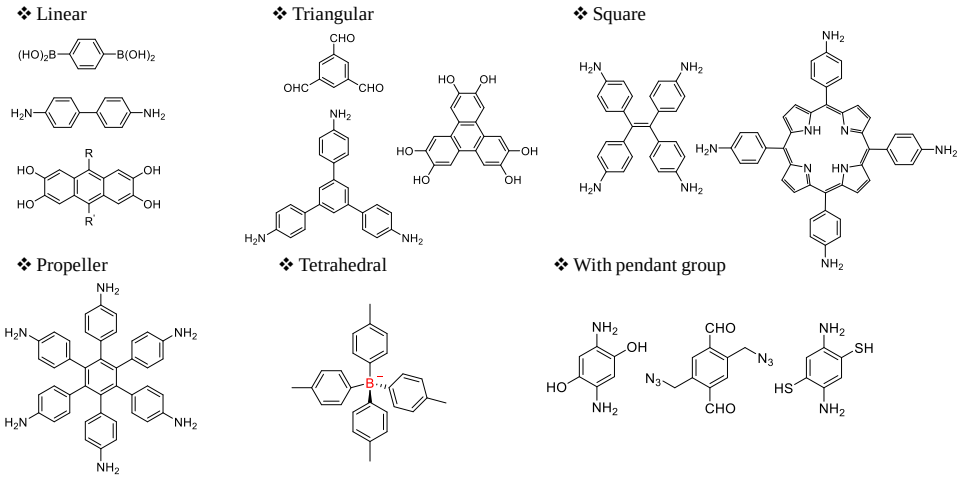

Figure 1. Some examples of building blocks or linker cores found in the COF skeleton.

Initially the first COFs were mainly synthesized using boronic ester linkages. However, due to their low stability under aqueous conditions[4], the major focus has shifted on to other forms of linkages like imine bonds[5], hydrazone bonds[6]; azine[7] and triazine[8][9] linkages; even oxazole, imidazole[10] and thiazole linkages have also made their way into the framework skeleton (**Figure 1**).

These covalent bonds typically result in COFs with a high mechanical, thermal, as well as chemical stability and their corresponding diverse structures of the building blocks make them highly tunable in terms of

topology, structure and functionality. The most important and distinguishable characteristic of COF is their free-adjustable porosity which is completely dependent on the length and geometry of the linkers used (**Figure 2**).

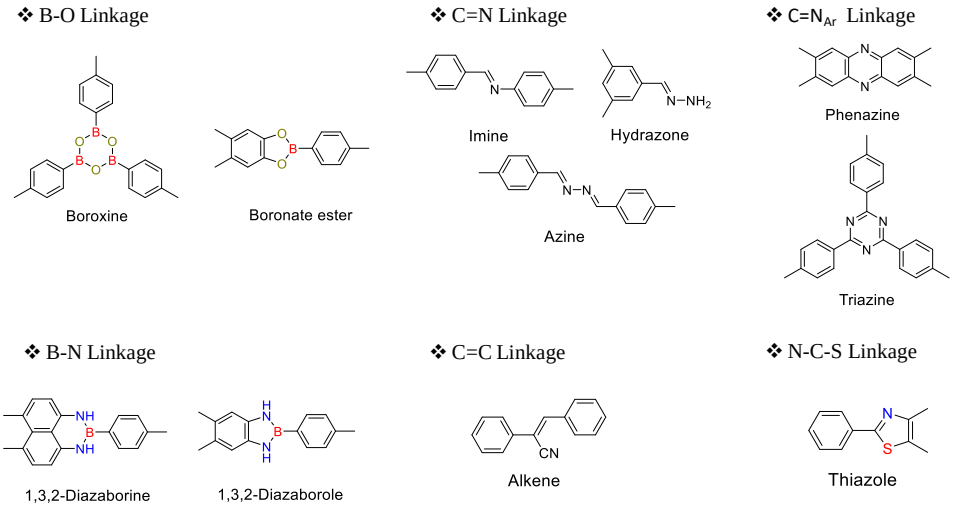

Figure 2. Examples of different linkers used in COF synthesis.

Incorporating the effects of dynamic covalent chemistry[2], π-π stacking interactions and intramolecular hydrogen bonding[3], a wide range of COFs have been designed till date. COFs are highly crystalline with intrinsic pore structures which have paved its way into applications in the fields of gas separation and storage; catalysis; energy storage; sensing and even in drug delivery (**Figure 3**).

From the point of view of the synthesis of these extended frameworks, the employment of dynamic covalent chemistry (DCC) plays a distinct role in formation of these beautifully extended and conjugated crystalline structures (**Figure 4**).

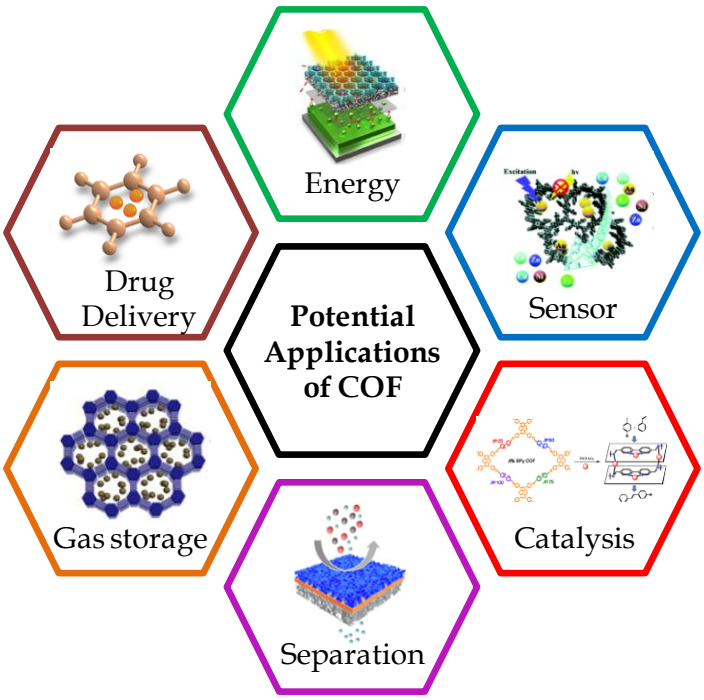

Figure 3. Various applications of COFs.

DCC refers to those reversible chemical reactions which are performed under equilibrium conditions[11][12]. During the formation of these covalent bonds, there may be generation of many unprecedented disordered covalent molecules with different free energies due to the randomness in the formation of these extended structures. Therefore, it becomes absolutely necessary to eliminate those kinetic products (polymers) which happens to be mostly amorphous in nature and hinders our framework growth. To overcome this problem, the condition of reversibility comes as a blessing in disguise as it imparts the properties of error correction and self-healing to our framework. Under these conditions of reversibility, even if any undesired bond formation takes place, the system can repair itself through bond breaking and subsequent bond reformation leading to our desired thermodynamic product (framework) with the lowest free energy. However given the strength of these covalent bonds are sufficiently high, the conditions of reversibility can only be employed under higher temperatures (120-180°C) and pressure. But the entire problem was still not solved as most of the organic building blocks usually

disintegrate at higher temperatures. To address this problem, scientists have tried to employ DCC induced by certain chemical reagents during the bond formation. Under this process a specific chemical agent (in most cases water) maintains the reversible chemical bond formation. Therefore the synthesis of these large molecules with a long range order is comparatively difficult as compared to the kinetic short range ordered polymers.

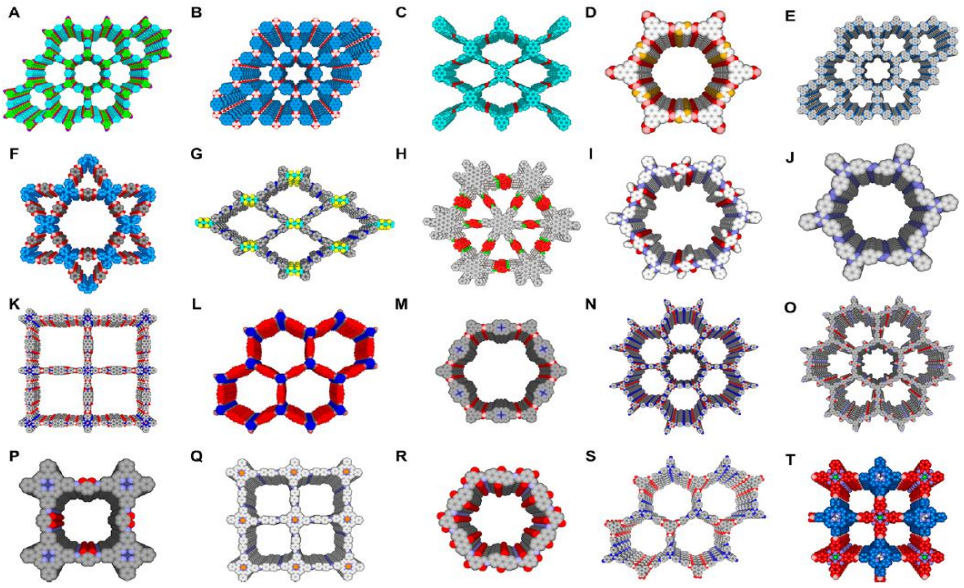

Figure 4. Examples of 2D COFs with layered stacking structures[13].

Chapter 2

PREVIOUS WORKS

2.1 Review of past works and project motivation.

The use of 'chemically induced Dynamic Covalent Chemistry' favored the synthesis of a wide variety of COF but it also had a downside. These frameworks so designed showed excellent stability towards a wide range of organic solvents. However under hydrolytic conditions, they were susceptible to decompose to its starting monomers following the Le Chateliar's principle as water is formed as a byproduct under these reversible conditions. Hence, the chemical stability of COF was pivotal for its application in different fields[14]. To address this issue, Banerjee *et al.* developed a novel synthetic route for the synthesis of a new library of crystalline and porous *β*-ketoenamine linked COF (**Figure 5**) which gains its stability through irreversible proton tautomerism[15].

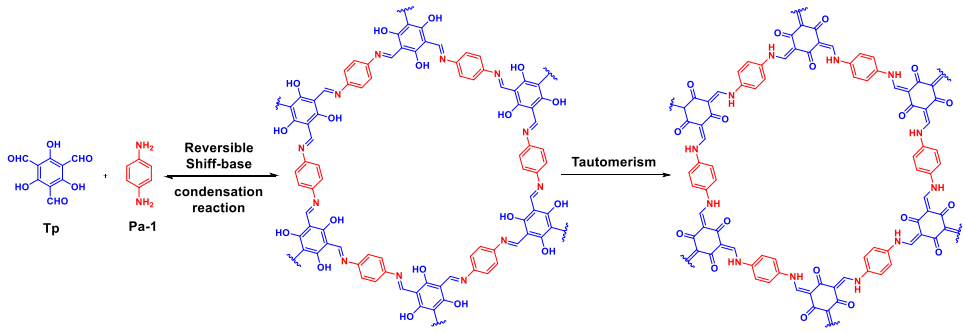

Figure 5. Schematic representation of the synthesis of COF **TpPa-1** by the combined reversible and irreversible cascade reaction of *p*-phenylenediamine with 1,3,5-triformylphloroglucinol[15].

A similar strategy was introduced by Wang *et al.* in 2018 using a similar reversible-irreversible cascade reaction to synthesize a benzoxazole linked COF[16]. Here the presence of the benzoxazole moiety not only offers extra stability to the COF structure but also provides extensive π-conjugation

which decreases its band gap and imparts enhanced photo-catalytic activity to the COF (**Figure 6**).

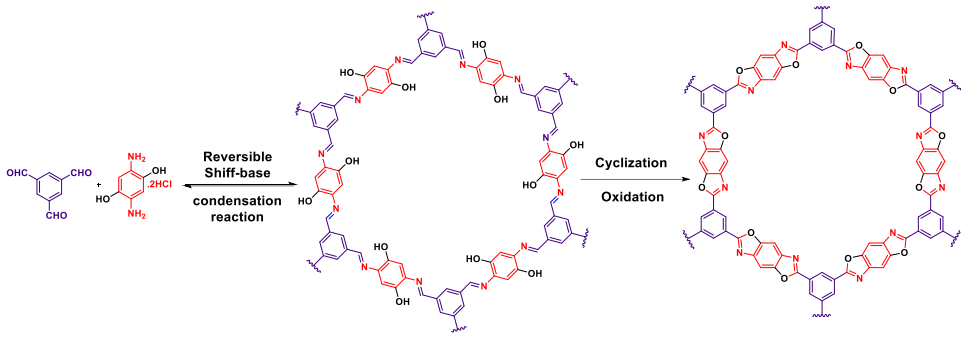

Figure 6. Synthesis of benzoxazole linked COF (**LZU-190**) via the cascade reaction between 1,3,5-triformylbenzene and 2,5-Diaminobenzene-1,4-diol dihydrochloride[16].

After the successful incorporation of benzoxazole fragment into the framework, Yaghi *et al.* extended the work on benzoxazole and went on to further include benzothiazole moiety into the COF structure via substitution of the linkers[17]. Since then various groups around the world has been synthesizing COF with bis-benzothiazole linkage via various methods.

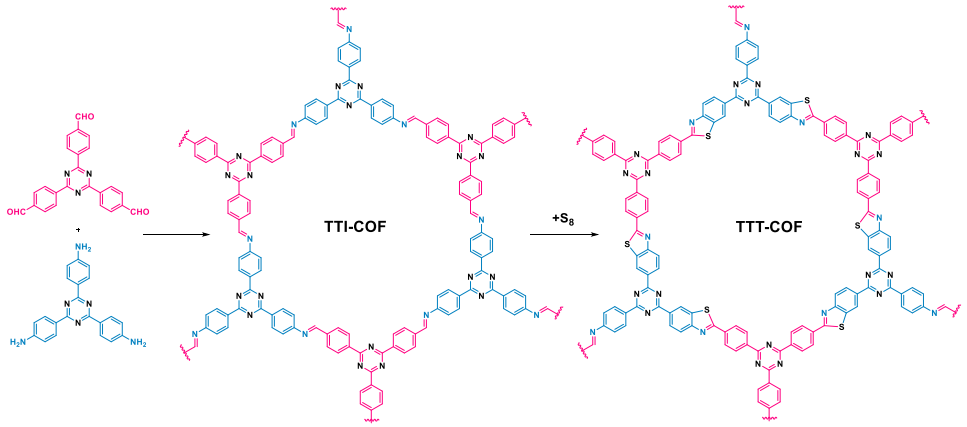

Figure 7. Synthesis of benzothiazole linked **TTT-COF**[18] from imine linked **TTI-COF**[19] using elemental sulphur for post synthetic modification.

Lotsch and her co-workers introduced a new method of incorporating benzothiazole moiety in the COF structure[18]. A post-synthetic modification was performed using elemental sulphur. Initially a imine based COF was synthesized using standard reported procedures[19] and then at higher temperatures, elemental sulphur reacts with the imine to oxidize it into thioamide which undergoes subsequent oxidation followed by cyclization to form the thiazole ring (**Figure 7**).

This methodology yielded various COFs with high structural integrity and excellent crystallinity[20-23]. However, the direct synthesis of a COF having bis-benzothiazole linkage has been less explored as per the literature. Zhi Guo Gu and his co-workers synthesized the COFs (PG-BBT and BZ-BBT) via the reversible and irreversible cascade reaction without involving any post synthetic modification using neither elemental sulphur nor linker exchange method[24] (**Figure 8**).

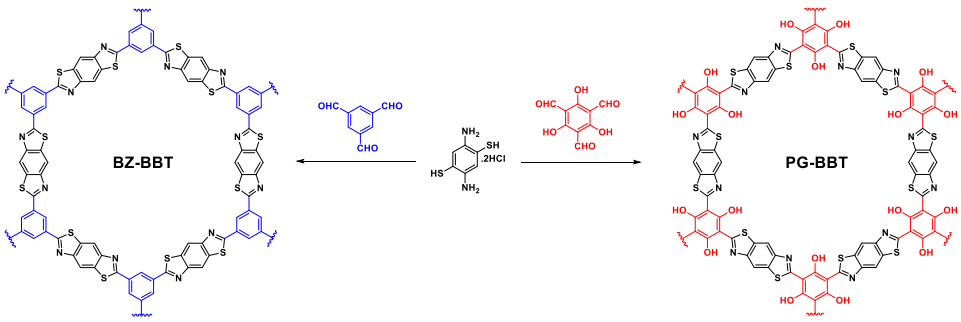

Figure 8. Synthesis of bis-benzothiazole linked COF **PG-BBT** and **BZ-BBT**[24].

Besides these strategies, various other methods and strategies has also been adopted in the past few years which gave rise to a large library of highly stable and crystalline COF.

So, our goal was to synthesize a stable bis-benzothiazole linked covalent organic framework, characterize it with the help of different spectroscopic techniques and utilize it for heterogeneous catalysis.

Chapter 3

REACTION SCHEMES

3.1 Reaction scheme 1

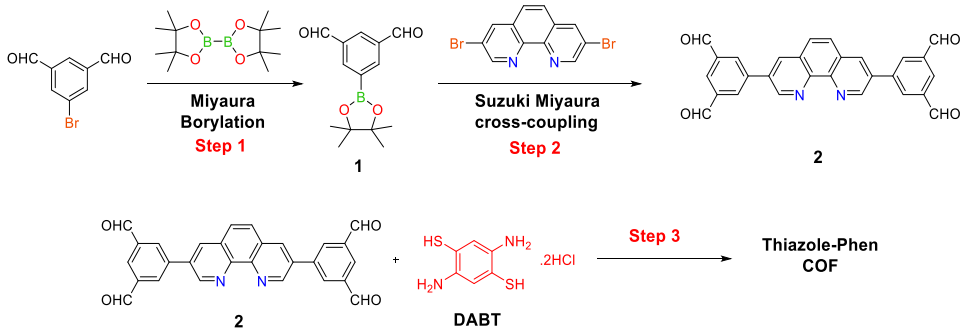

Scheme 1. Reaction scheme 1.

In the first step of this scheme, 5-(4,4,5,5-tetramethyl-1,3,2-dioxaborolan-2-yl) isophthalaldehyde (**1**) was synthesized by employing Miyaura borylation reaction using 5-bromoisophthaldehyde and bis(pinacolato)diboron. We further planned to synthesize 5,5'-(1,10-phenanthroline-3,8-diyl)diisophthalaldehyde i.e. compound **2** from compound **1** and 3,8-dibromo-1,10-phenanthroline utilizing Suzuki-Miyaura cross-coupling reaction. However due to solubility issues, compound **2** could not be characterized hence we shifted to scheme 2.

3.2 Reaction scheme 2

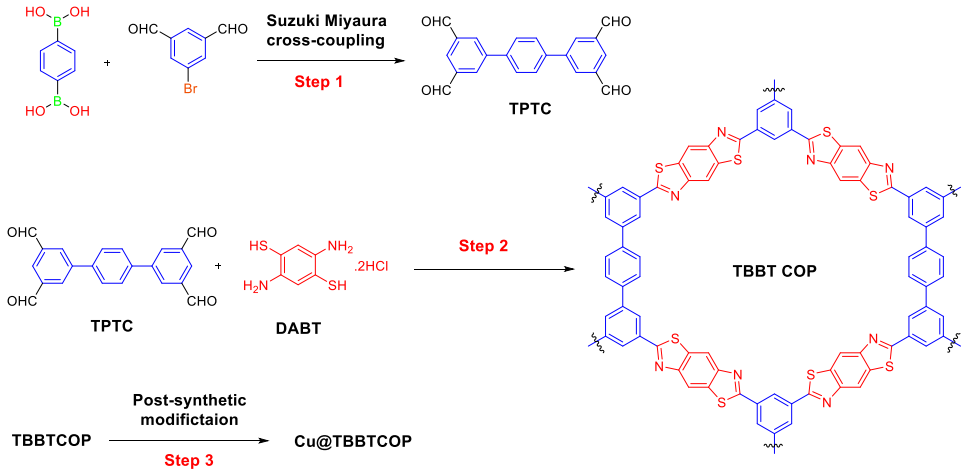

Scheme 2. Overall reaction scheme for the synthesis of TBBTCOP.

[1,1':4',1"-terphenyl]-3,3",5,5"-tetracarbaldehyde (TPTC) was synthesized from benzene-1,4-diboronic acid and 5-bromoisophthaldehyde employing Suzuki-Miyaura cross-coupling reaction. Using TPTC and 2,5-diamino-1,4-benzenedithiol dihydrochloride (DABT), TBBTCOP was synthesized under microwave irradiation. Further, post-synthetic modification was performed on our polymer by incorporating copper into its structure.

3.3 Chan-Lam coupling reaction using Cu@TBBTCOP.

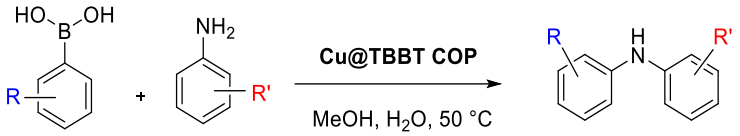

Scheme 3. General reaction scheme for C-N cross-coupling reaction.

Cu@TBBTCOP was further used for the Chan-Lam coupling reaction between arylboronic acid arylamine derivatives.

3.4 Metal free C-C coupling reaction using TBBTCOP.

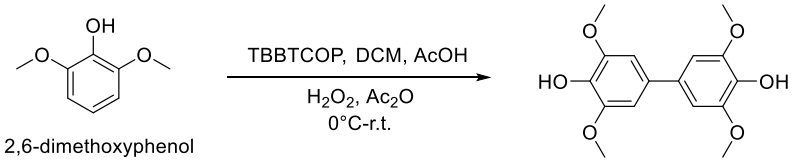

Scheme 4. General reaction scheme for the metal free C-C coupling reaction.

We also tried to perform the metal free C-C coupling reaction using TBBTCOP using phenol derivatives.

Chapter 4

EXPERIMENTAL SECTION

4.1 Materials required

All the chemicals and reagents were purchased from commercially available sources like Alfa Aesar, BLD Pharmatech Pvt. Ltd., SRL Pvt. Ltd., TCI Co., Ltd., FINAR Ltd., Sigma-Aldrich-India and Merck.

2,5-diamino-1,4-benzenedithiol dihydrochloride, 3,8-dibromo-1,10-phenanthroline, 5-bromoisophthaldehyde were purchased from BLD Pharmatech Pvt. Ltd. Benzene-1,4-diboronic acid and bis(pinacolato)diboron were purchased from Alfa Aesar. Ascorbic acid and $NaBH_4$ were purchased from Sigma-Aldrich-India. $Pd(PPh_3)_4$, $Pd(dppf)Cl_2$ and $Pd(PPh_3)_2Cl_2$ were purchased from TCI Co., Ltd. Anhydrous Na_2SO_4, Na_2CO_3, KOAc, K_2CO_3, K_3PO_4, aniline, phenylboronic acid and *m*-toluidine were purchased from SRL Pvt. Ltd. Methanol, DMF, THF, 1,4-dioxane, diethyl ether, TFA and NMP were purchased from Merck, ethyl acetate, DCM, chloroform, ethanol and hexane were purchased from FINAR Ltd. Methanol, ethyl acetate, DCM, chloroform, 1,4-dioxane and hexane were purified using distillation process prior to their use in reactions.

4.2 General

^{1}H and ^{13}C NMR spectra of all the precursors and final compounds were recorded on Bruker AV 500 MHz instrument using tetramethylsilane as the internal standard and $CDCl_3$ as solvent with the solvent residual peak at δ 7.26 ppm. Thin-layer chromatography was performed on pre-coated silica gel plates (Kieselgel 60 F_{254}, Merck). The precursors were purified by Flash Chromatography (TELEDYNE ISCO, USA; model: CombiFlash®Rf+) using silica gel (100-200 mesh) with DCM/hexane (ratio as required) as eluent. Monowave 200 autosampler MAS 24 by

Anton Paar was used for synthesis of our polymer. FTIR spectra of the compounds were acquired on Bruker (tensor 27) FT-IR spectrometer in the range from 4000-400 cm^{-1}. Powder XRD patterns were collected from $2\theta = 2°$ to 60° on Rigaku SmartLab, an Automated Multipurpose X-ray Diffractometer. Thermogravimetric analysis (TGA) was analyzed using Mettler Toledo Thermal Analyzer with a heating rate of 10 °C/min. BET surface area was analyzed on Quantachrome, Autosorb iQ2. Morphological studies were carried out by FE-SEM analysis. Field emission scanning electron microscopic images were obtained using a Supra 55 Zeiss.

4.3 Synthesis of compounds

4.3.1 Synthesis of 5-(4,4,5,5-tetramethyl-1,3,2-dioxaborolan-2-yl) isophthalaldehyde (**1**)

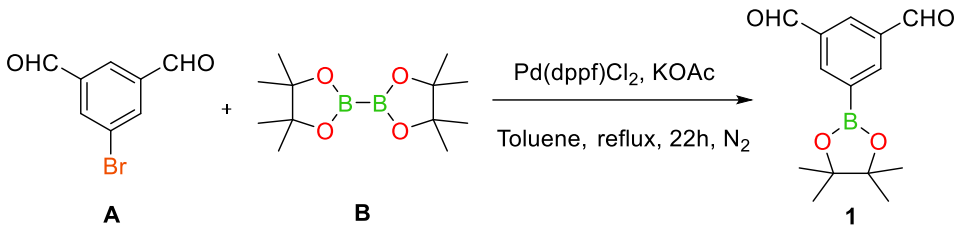

Scheme 5. Synthesis of compound **1**

A 100 mL R.B. flask was charged with a solution of 5-bromoisophthaldehyde (0.430 g, 2.018 mmol, 1 equiv.), bis(pinacolato)diboron (0.564 g, 2.2198 mmol, 1.1 equiv.) and KOAc (0.625 g, 6.368 mmol, 3.2 equiv.) in anhydrous toluene (15 mL) followed by addition of $Pd(dppf)Cl_2$ (73.8 mg, 0.1009 mmol, 0.05 equiv.). The temperature of the reaction was raised upto 100 °C and stirred for 22 h. Then the solution was cooled and dried under vacuum and extracted with diethyl ether. The extract was passed through celite (size 20-40 μm) bed and then washed with brine solution (4 x 20 mL) and deionized water (4 x 20 mL) and dried over Na_2SO_4. The extract was then concentrated under vacuum and purified by flash chromatography with 90% DCM in hexane as eluent to obtain a white crystalline product.

Yield: 75% (0.395 g, 1.52mmol)

^{1}H NMR (500 MHz, $CDCl_3$): δ 1.38 (s, 12H), 8.46 (s, 1H), 8.55 (s, 2H), 10.13 (s, 2H) ppm

^{13}C NMR (125 MHz, $CDCl_3$):δ 25.0, 84.9, 128.6, 132.3, 136.5, 141.5, 191.4 ppm

4.3.2 Synthesis of 5,5'-(1,10-phenanthroline-3,8-diyl)diisophthalaldehyde (**2**)

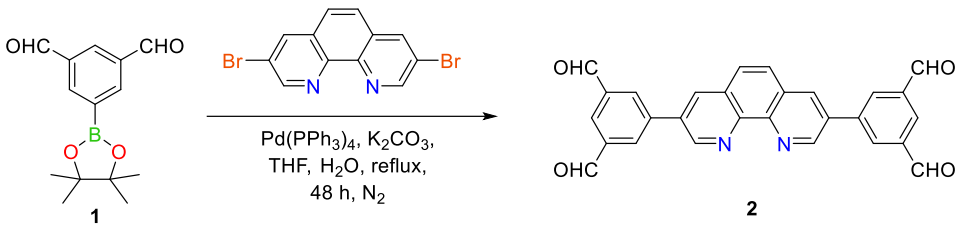

Scheme 6. Synthesis of compound **2**.

$Pd(PPh_3)_4$ (0.019 g, 0.0163 mmol, 0.05 equiv.) was added to a two neck R.B. and dry purged with nitrogen for 5 min. To it, THF (13.5 mL) was added under inert atmosphere and left to stir for 10 min. After the time elapsed, K_2CO_3 (0.162 g, 1.172 mmol, 3.6 equiv.) and 3,8-dibromo-1,10-phenanthroline (0.110 g, 0.325 mmol, 1 equiv.) was added. After stirring for another 15 min, compound **1** (0.178 g, 0.683 mmol, 2.1 equiv.) and water (1.5 mL) was added. The temperature of the reaction was raised upto 90 °C under reflux and stirred for 48 h. After the reaction was complete, the precipitate formed was filtered and washed with ether (100 mL), water (100 mL) and again with ether (100 mL) and dried overnight to obtain a yellow solid.

4.3.3 Synthesis of [1,1':4',1''-terphenyl]-3,3'',5,5''-tetracarbaldehyde (TPTC).

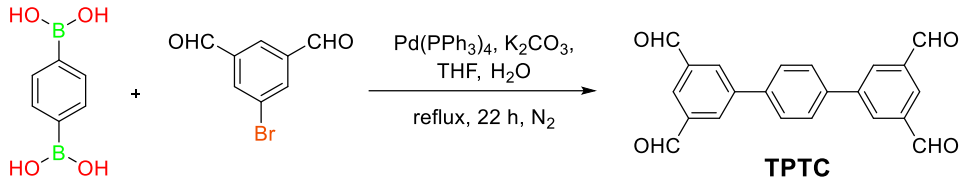

Scheme 7. Synthesis of TPTC.

$Pd(PPh_3)_4$ (0.069 g, 0.06 mmol, 0.05 equiv.) was added to a two neck R.B. and dry purged with nitrogen for 5 min. To it, THF (10 mL) was added under inert atmosphere and left to stir for 10 min. After the time elapsed, 5-bromoisophthaldehyde (0.771 g, 3.62 mmol, 3.0 equiv.) was added followed by addition of K_2CO_3 (1.668 g, 12.07 mmol, 10.0 equiv). To dissolve the base, water (10 mL) was added. After stirring for another 15 min, benzene-1,4-diboronic acid (0.2 g, 1.207 mmol, 1.0 equiv.) and THF (10 mL) was further added. The temperature of the reaction was raised upto 80 °C and stirred under reflux for 22 h. After the reaction was complete, the precipitate formed was filtered and washed with ether (100 mL), water (100 mL) and again with ether (100 mL) and dried overnight at 60 °C to obtain our desired compound as a light grey solid.

Yield: 81% (0.335 g, 0.98 mmol)

^{1}H NMR (500 MHz, $CDCl_3$+CF_3COOH): δ 7.88 (s, 4H), 8.53 (s, 2H), 8.57 (s, 4H), 10.13 (s, 2H) ppm

^{13}C NMR (125 MHz, $CDCl_3$+CF_3COOH): δ 128.1, 131.6, 134.5, 136.8, 138.3, 142.9, 194.4 ppm

4.3.4 Synthesis of TBBTCOP.

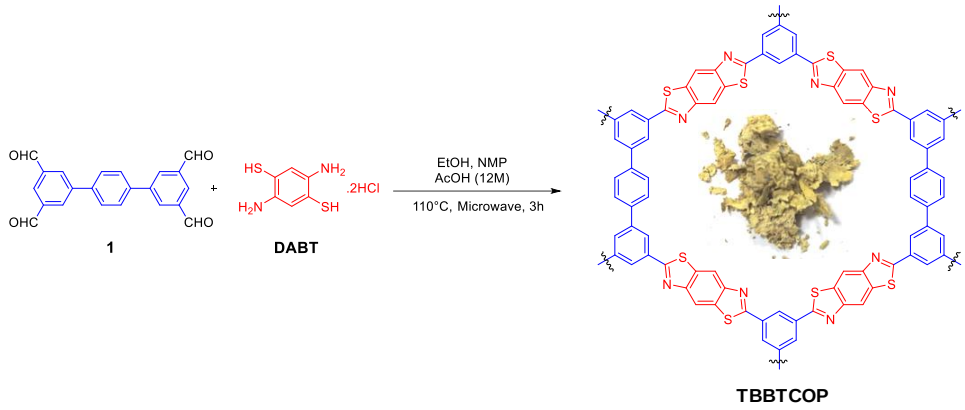

Scheme 8. Synthesis of TBBTCOP.

In a 10 mL microwave glass vial, DABT (0.043 g, 0.174 mmol, 3 equiv.) was dissolved in ethanol (1 mL). TPTC (0.02 g, 0.058 mmol, 1 equiv) dissolved in NMP (2 mL) was added to the solution followed by addition of 0.1 mL of 12 M AcOH. The contents in the glass vial were purged with N_2, capped and then placed in a microwave reactor for 3 h maintaining the temperature at 110 °C. After the elapsed time, the precipitate was filtered and washed with DMF, THF, acetone, water and methanol in this order. It was then dried at 100 °C under vacuum for 12 h to obtain TBBTCOP as a pale green powder.

4.3.5 Synthesis of Cu@TBBTCOP (Method 1).

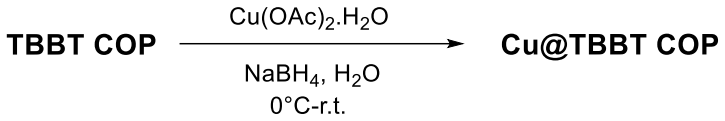

Scheme 9. Synthesis of Cu@TBBTCOP – Method 1.

20 mg of TBBTCOP was dispersed into 20 mL D.I. water in a 100 mL two neck R.B. flask. This was followed by addition of 10 mL of 20 mM solution of copper acetate monohydrate. The reaction was continued in the dark for 5 h at 0 °C. After 5 h, reaction mixture was centrifuged to separate out the copper ion incorporated COP from the solution. The COP was further redispersed into 20 mL D.I. water and 10 mL solution of aqueous sodium borohydride (30 mM) was added slowly for 20 minutes maintaining ice cold condition. The reaction was further continued for 2 h at 0 °C and finally at room temperature for overnight under dark conditions. The copper incorporated COP was washed with water and dried at 70 °C for 12 h to obtain as a dark green solid.

4.3.6 Synthesis of Cu@TBBTCOP (Method 2).

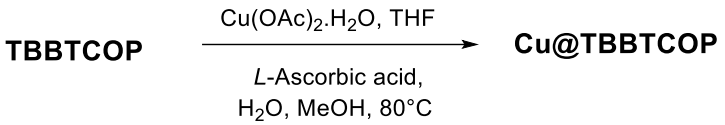

Scheme 10. Synthesis of Cu@TBBTCOP – Method 2.

40 mg of TBBTCOP was dispersed into 15 mL dry THF in a 100 mL two neck R.B. flask. This was followed by addition of 5 mL of 100 mM solution of copper acetate monohydrate. The reaction was stirred for 12 h at room temperature. After the elapsed time, the reaction mixture was filtered and thoroughly washed with methanol and D.I. water. The COP was further redispersed into a solution of water and methanol (3:1) mixture and was stirred under inert atmosphere. This was followed by addition of 5 mL, 1.0 M solution of ascorbic acid maintaining the inert atmosphere. The temperature of the reaction mixture was raised to 80 °C and was stirred for 24 h. The copper incorporated TBBTCOP was washed with water and methanol and dried at 70 °C for 12 h to obtain as a dark green solid.

4.3.7 Utilization of TBBTCOP for metal free C-C coupling reaction.

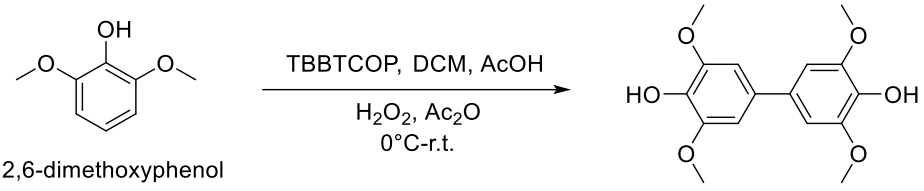

Scheme 11. C-C coupling reaction of 2,6-dimethoxyhenol.

TBBTCOP (10 mg) was added to a solution of DCM (1 mL) and acetic acid (1 mL) in a 20 mL reaction tube. The temperature of the reaction mixture was reduced down to 0 °C and H_2O_2 (0.04 mL, 1.68 mmol, 8 equiv.) and Ac_2O (0.16 mL, 1.68 mmol, 8 equiv.) were added in five portions over a period of 2 h. 2,6-dimethoxyhenol (0.033 g, 0.21 mmol, 1 equiv.) was added and the reaction was continued for 2 days at r.t. After the elapsed time, the reaction mixture was filtered and the filtrate was concentrated under rota. The crude was further extracted with ethyl acetate and was washed with brine, water and dried over Na_2SO_4.

4.3.8 Utilization of Cu@TBBTCOP for Chan-Lam coupling reaction.

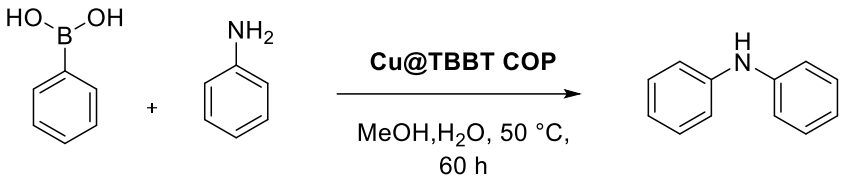

Scheme 12.C-N coupling reaction between phenylboronic acid and aniline.

Cu@TBBTCOP (10 mg) was taken in a 20 mL reaction tube. Phenylboronic acid (0.092 g, 0.75 mmol, 1.5 equiv.) dissolved in 2 mL MeOH was added to the reaction tube containing the COP. Aniline (0.046 mL, 0.5 mmol, 1 equiv.) was added followed by addition of 1 mL of D.I. water. The reaction was stirred for 60 h at 50 °C and was monitored by TLC. After completion of the reaction, the contents of the reaction were filtered and extracted with ethyl acetate. The extract was further washed with brine (4 x 20 mL) and dried over Na_2SO_4. The extract was then concentrated under vacuum and purified by flash chromatography with 10% ethyl acetate in hexane as eluent to obtain a yellowish product.

Yield: 73% (0.062 g, 0.366 mmol)

Chapter 5

RESULTS AND DISCUSSION

5.1 Characterization

5.1.1 ^{1}H and ^{13}C NMR spectra of scheme 1.

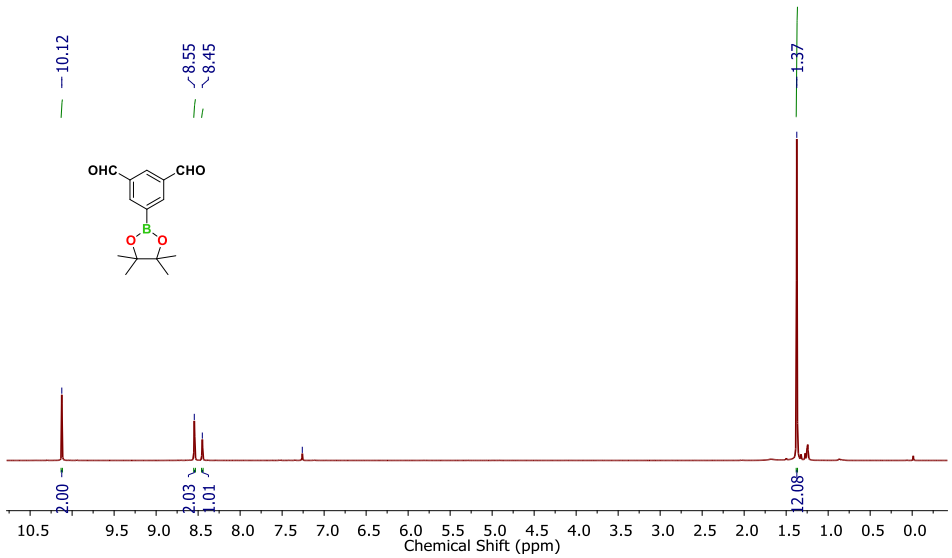

Figure 9. ^{1}H NMR (500 MHz, $CDCl_3$) spectrum of compound **1**.

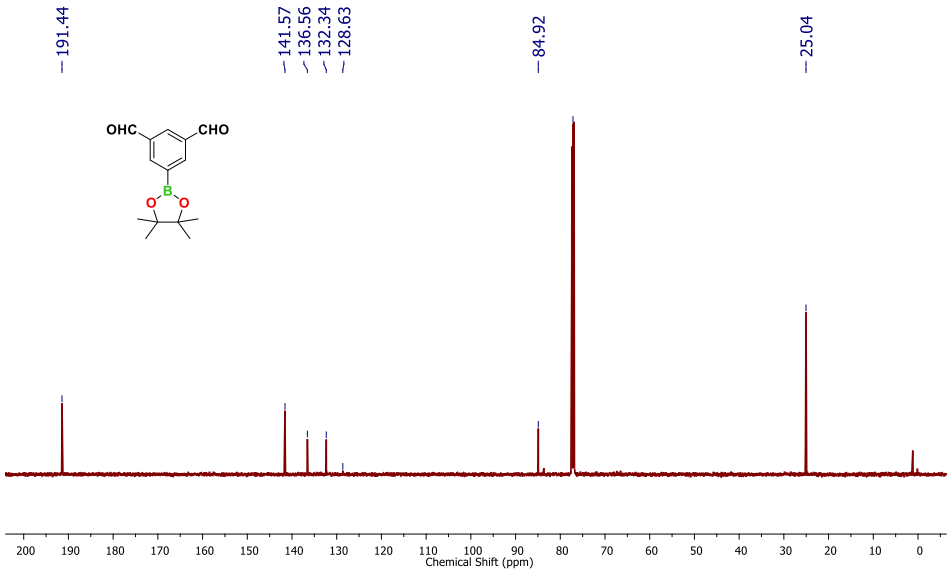

Figure 10. ^{13}C NMR (500 MHz, $CDCl_3$) spectrum of compound **1**.

5.1.2 ^{1}H and ^{13}C NMR spectra of scheme 2.

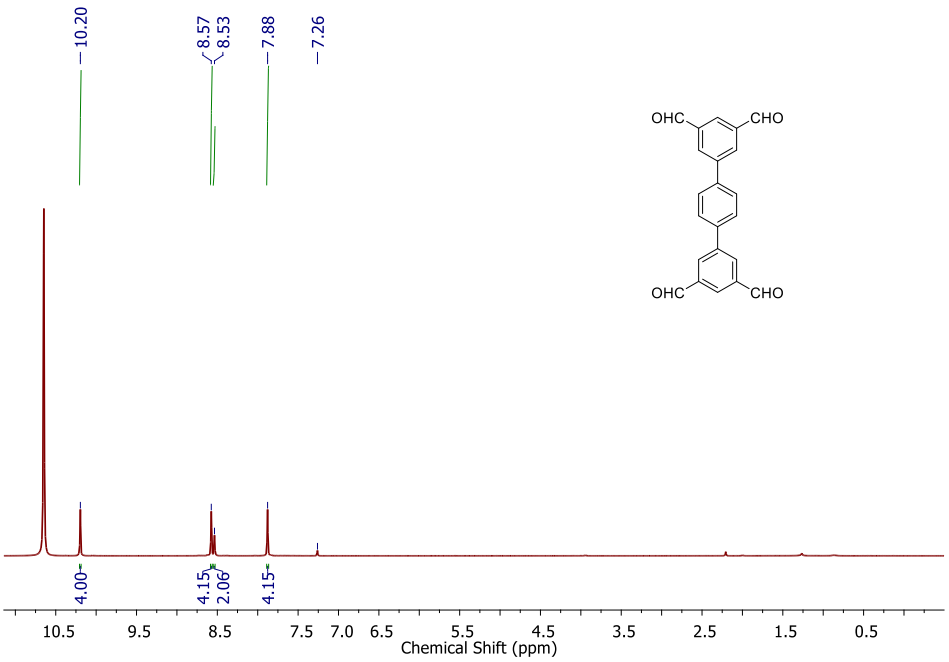

Figure 11. ^{1}H NMR (500 MHz, $CDCl_3$+CF_3COOH) spectrum of TPTC.

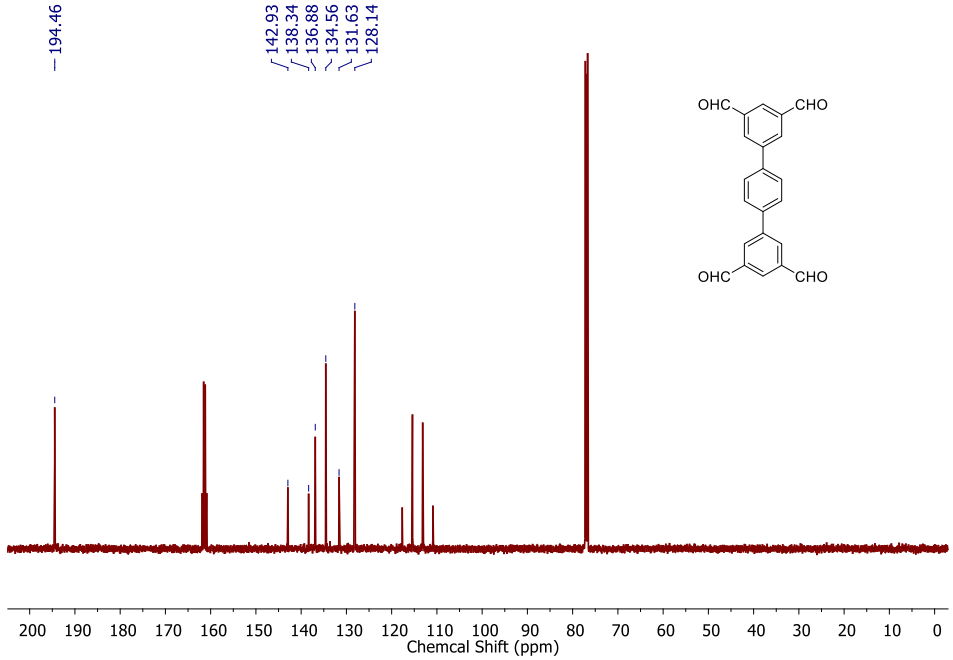

Figure 12. ^{13}C NMR (125 MHz, $CDCl_3$+CF_3COOH) spectrum of TPTC.

5.1.3 Characterization of TBBTCOP.

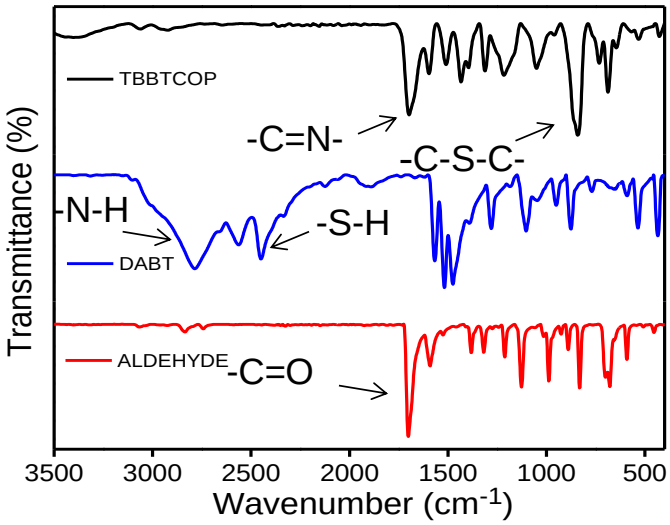

Figure 13. FT-IR spectra of TBBTCOP.

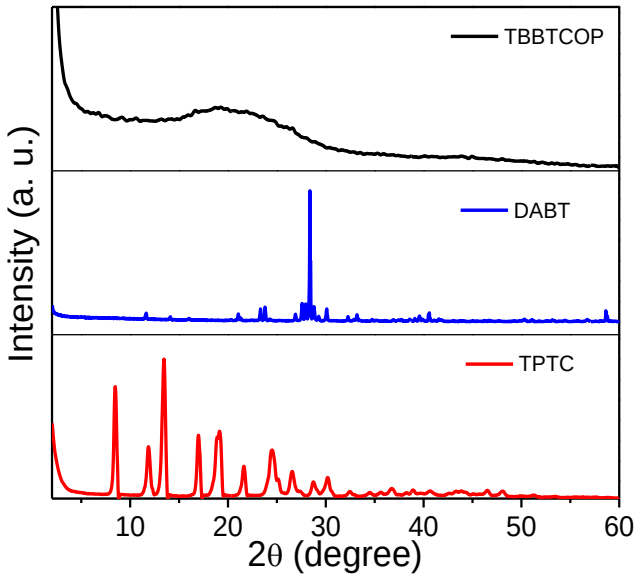

Figure 14. PXRD spectra of TBBTCOP.

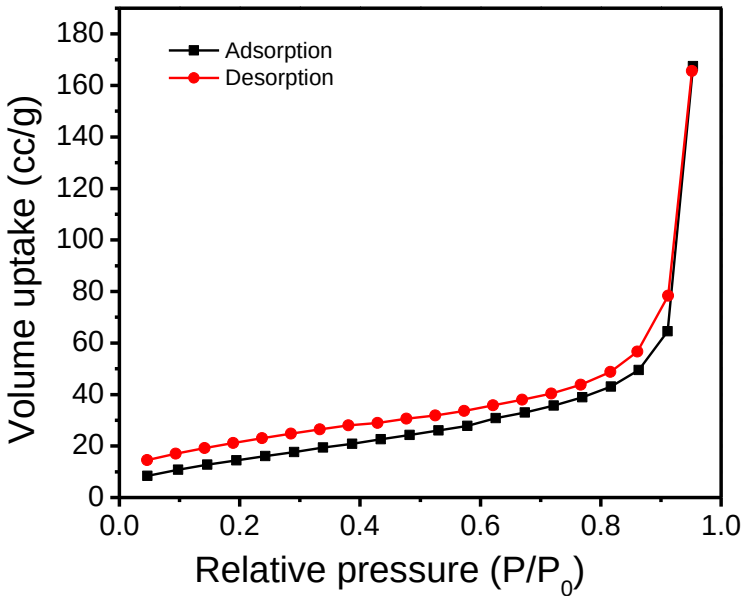

Figure 15. N_2 adsorption-desorption isotherm of TBBTCOP.

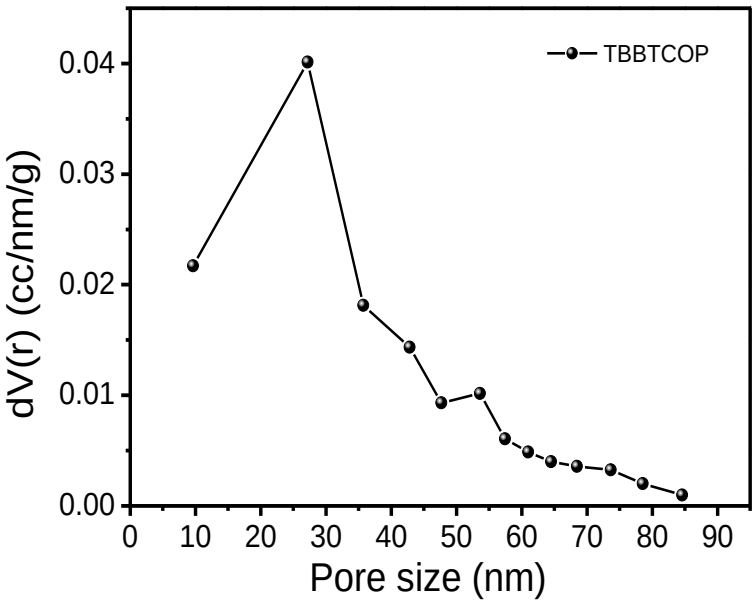

Figure 16. Pore size distribution of TBBTCOP.

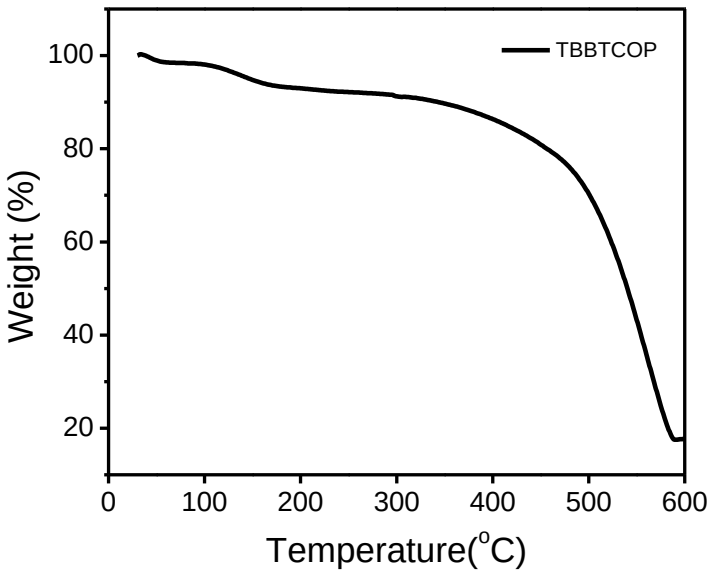

Figure 17. TGA analysis of TBBTCOP.

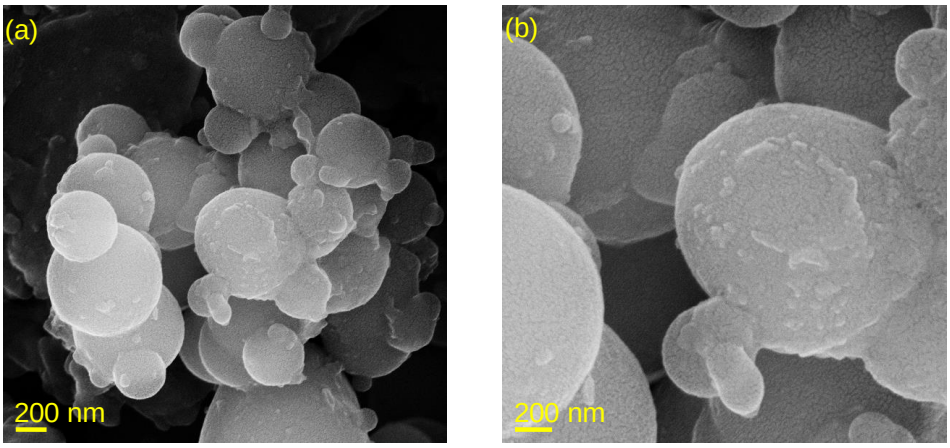

Figure 18. FE-SEM images of TBBTCOP.

5.1.4 Characterization of Cu@TBBTCOP.

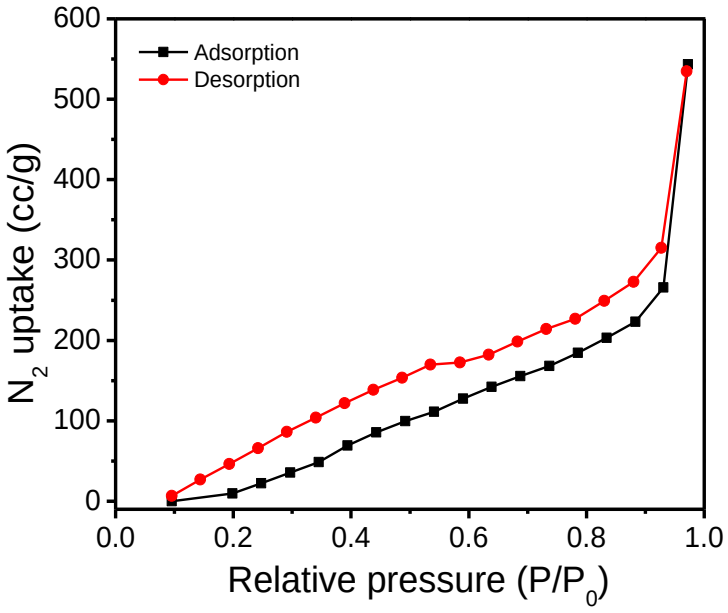

Figure 19. N_2 adsorption-desorption isotherm of Cu@TBBTCOP.

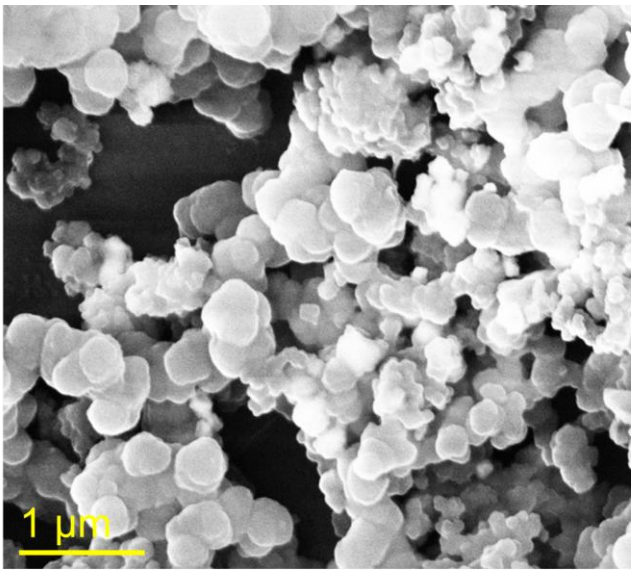

Figure 20. FE-SEM images of Cu@TBBTCOP.

5.2 Synthesis of compound 1.

Initially, for the synthesis of compound **1** we tried to perform the controlled oxidation of 3,5-dimethylphenyl-boronic acid pinacol ester using oxidizing agents such as MnO_2 and SeO_2 respectively. In case of oxidation using manganese dioxide, the ^1H NMR spectra of the crude showed a small peak at δ 10.2 (s) ppm which may correspond to aldehyde proton peak. However, there was a significant crowding in the aromatic region which may suggest the deprotection of the boronic ester group under acidic condition. In the later case, oxidation using selenium dioxide poses an even greater issue as a new broad singlet peak appears in the ^1H NMR spectra at δ 3.77 ppm instead of the characteristic aldehydic proton peak within δ 9-10.5 ppm. So both these methodologies were proved to be inefficient for the synthesis of compound **1**. We then tried to perform Miyaura borylation of 5-bromoisophthaldehyde with bis(pinacolato)diboron, KOAc and $Pd(dppf)Cl_2$. The NMR of the compound after purification showed distinct peaks for the aldehyde as well as for the boronic acid pinacol ester and upon further optimization, compound **1** was obtained with good yields.

Table 1. Optimization table for the synthesis of compound **1**.

Sr. No	Compound A	Compound B	Catalyst	Base	Solvent	Temperature (°C)	Time	Yield (%)
1.	1.0 equiv.	1.1 equiv.	$Pd(dppf)Cl_2$ (0.05 equiv.)	KOAc (3 equiv.)	1,4-dioxane	90	22 h	15
2.	1.0 equiv.	1.1 equiv.	$Pd(dppf)Cl_2$ (0.05 equiv.)	KOAc (4 equiv.)	1,4-dioxane	90	70 h	25
3.	1.0 equiv.	1.1 equiv.	$Pd(dppf)Cl_2$ (0.05 equiv.)	KOAc (3 equiv.)	1,4-dioxane	100	24 h	55
4.	1.0 equiv.	1.1 equiv.	$Pd(dppf)Cl_2$ (0.05 equiv.)	KOAc (4 equiv.)	1,4-dioxane	100	22 h	39
5.	1.0 equiv.	1.1 equiv.	$Pd(dppf)Cl_2$ (0.05 equiv.)	KOAc (3.2 equiv.)	Toluene	105	22 h	75

5.3 Synthesis of compound 2.

For our second step, we have tried to perform the reaction several times by modifying the reaction conditions; however we were still not able to purify and isolate our desired compound yet. A noticeable outcome which was observed in all the reaction was the formation of a by-product in the form of isophthaldehyde. The ^{1}H and ^{13}C NMR study also confirms its formation. The major problem in this synthesis was the solubility of our desired compound **2**. During the course of the reaction, it precipitates out from the reaction mixture and even after the process of filtration and washing we could not obtain the NMR of compound **2**.

5.4 Synthesis of TPTC.

TPTC was synthesized from benzene-1,4-diboronic acid and 5-bromoisophthaldehyde via Suzuki-Miyaura cross coupling reaction. Since TPTC was only partially soluble in NMP and DMF. So in order to characterize our compound using NMR, we added a very small amount of trifluoro acetic acid (20 µL) to solubilize our compound (20 mg). Hence we obtain an extra peak at δ 10.7 in the ^{1}H NMR spectrum (**Figure 11**) and two extra peaks in the ^{13}C NMR spectrum which corresponds to the peaks of TFA (**Figure 12**).

5.5 Synthesis of TBBTCOP.

We tried out several experiments by varying the concentration, solvent system and even the mode of heating for optimization of the conditions for the synthesis of our polymer.

Among all the performed conditions, we obtained the most satisfactory result when the reaction was performed under the conditions mentioned in entry 17 of table 2.

Table 2. Optimization table for the synthesis of TBBTCOP.

Sr. No	TPTC	DABT	Catalyst (AcOH)	Solvent system	Method of heating	Temperature (°C)	Time	Description of polymer
1.	1.0 equiv.	2.0 equiv.	6 M, 0.2 mL	Mesitylene: 1,4-dioxane (1:6)	R.B. with reflux	120	72 h	**Yellowish green powder**
2.	1.0 equiv.	2.0 equiv.	6 M, 0.2 mL	Mesitylene: 1,4-dioxane (1:6)	Sealed tube	120	72 h	**Brown powder**
3.	1.0 equiv.	2.0 equiv.	6 M, 0.2 mL	Mesitylene: 1,4-dioxane (1:6)	Sealed R.B.	120	72 h	**Dirty green powder**
4.	1.0 equiv.	2.0 equiv.	6 M, 0.2 mL	Mesitylene: 1,4-dioxane (1:6)	Oven	120	72 h	**Dirty green powder**
5.	1.0 equiv.	2.0 equiv.	6 M, 0.2 mL	Mesitylene: 1,4-dioxane (1:6)	Microwave	100	1 h	**Brown powder**
6.	1.0 equiv.	2.0 equiv.	6 M, 0.2 mL	Mesitylene: 1,4-dioxane (1:6)	R.B. with reflux	120	120 h	**Dirty green powder**
7.	1.0 equiv.	2.0 equiv.	6 M, 0.2 mL	DMF	Microwave	120	2 h	**Green powder**
8.	1.0 equiv.	2.0 equiv.	Nil	DMF	Microwave	120	2 h	**Yellowish green powder**
9.	1.0 equiv.	2.0 equiv.	6 M, 0.2 mL	Mesitylene: 1,4-dioxane (1:6)	Microwave	100	2 h	**Dirty green powder**
10.	1.0 equiv.	2.0 equiv.	6 M, 0.2 mL	DMF	Microwave	100	2 h	**Yellowish green powder**

Sr. No	TPTC	DABT	Catalyst (AcOH)	Solvent system	Method of heating	Temperature (°C)	Time	Description of polymer
11.	1.0 equiv.	2.0 equiv.	6 M, 0.2 mL	Mesitylene: DMF (1:1)	Microwave	100	2 h	**Yellowish green powder**
12.	1.0 equiv.	2.0 equiv.	6 M, 0.2 mL	NMP	Sealed tube	120	72 h	**Yellow powder**
13.	1.0 equiv.	3.0 equiv.	6 M, 0.2 mL	NMP:1,4-dioxane (1:1)	Microwave	100	2 h	**Green powder**
14.	1.0 equiv.	3.0 equiv.	6 M, 0.2 mL	Mesitylene: DMF (1:1)	Microwave	100	2 h	**Yellowish green powder**
15.	1.0 equiv.	3.0 equiv.	12 M, 0.2 mL	NMP:ACN (1:1)	Microwave	100	2 h	**Yellowish green powder**
16.	1.0 equiv.	3.0 equiv.	12 M, 0.2 mL	NMP:EtOH (1:1)	Microwave	110	3 h	**Green powder**
17.	1.0 equiv.	3.0 equiv.	12 M, 0.1 mL	NMP:EtOH (2:1)	Microwave	110	3 h	**Pale green powder**
18.	1.0 equiv.	3.0 equiv.	12 M, 0.4 mL	Mesitylene: NMP (1:1)	Microwave	120	3 h	**Brownish green powder**
19.	1.0 equiv.	3.0 equiv.	12 M, 0.1 mL	Mesitylene: NMP: DMSO (1:1:1)	Microwave	140	3 h	**Light brown powder**
20.	1.0 equiv.	3.0 equiv.	6 M, 0.1 mL	Mesitylene: DMF (1:1)	Microwave	100 150	1 h 3 h	**Pale green powder**

The formation of our polymer was confirmed by FT-IR study (**Figure 13**). The disappearance of the peak at 1706 cm^{-1} corresponding to the carbonyl stretching frequency of TPTC and 2500-3200 cm^{-1} corresponding to N-H and S-H stretching frequencies and appearance of new peaks at 1660 cm^{-1} (-C=N- stretching) and at 830 cm^{-1} (C-S-C stretching) provides evidences for the successful synthesis of our designed COP. The PXRD analysis (**Figure 14)** shows the amorphous nature of our synthesized TBBTCOP and the FE-SEM analysis shows its spherical morphology (**Figure 18**). The nitrogen sorption analysis was performed at 77 K and 1 bar pressure to analyze the porosity and surface area of TBBTCOP. As per the results, TBBTCOP exhibits a type IV isotherm with the surface area of 41.96 $m^2 g^{-1}$. The average pore size of TBBTCOP was calculated to be 3.5 nm using the BJH method with an average pore volume of 0.25 cc g^{-1}, thus indicating the mesoporous nature of our COP.

5.6 Time dependent study of TBBTCOP.

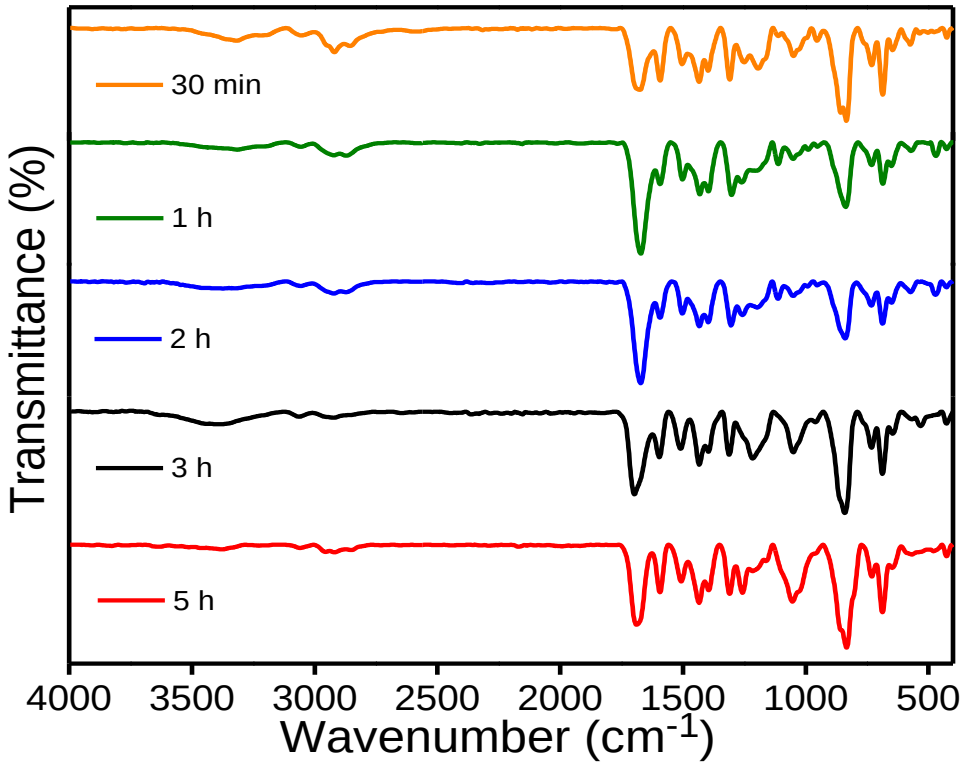

Figure 21. Time dependent study of TBBTCOP in different solvents.

To understand the change in the overall structure of the TBBTCOP during its formation, we performed the time dependent study during its synthesis. To perform the analysis, 10 mg of crude was collected during the synthesis process at the following tie intervals: 30 min, 60 min, 2 h, 3 h and 5 h. Initially after 30 min, the FT-IR recorded showed the presence of residual stretching frequency for –N-H and –S-H along with the peak for –C=O. However, with the passage of time, the intensity of the stretching frequencies of the monomers gradually decreased and stretching frequency for –C=N and –C-S-C increased significantly. Again the best results were obtained at 3 h and 5 h. But since, there was no significant change in the IR on going from 3 h to 5 h, hence 3 h was the optimized time that we took for the synthesis of TBBTCOP.

5.7 Stability test of TBBTCOP.

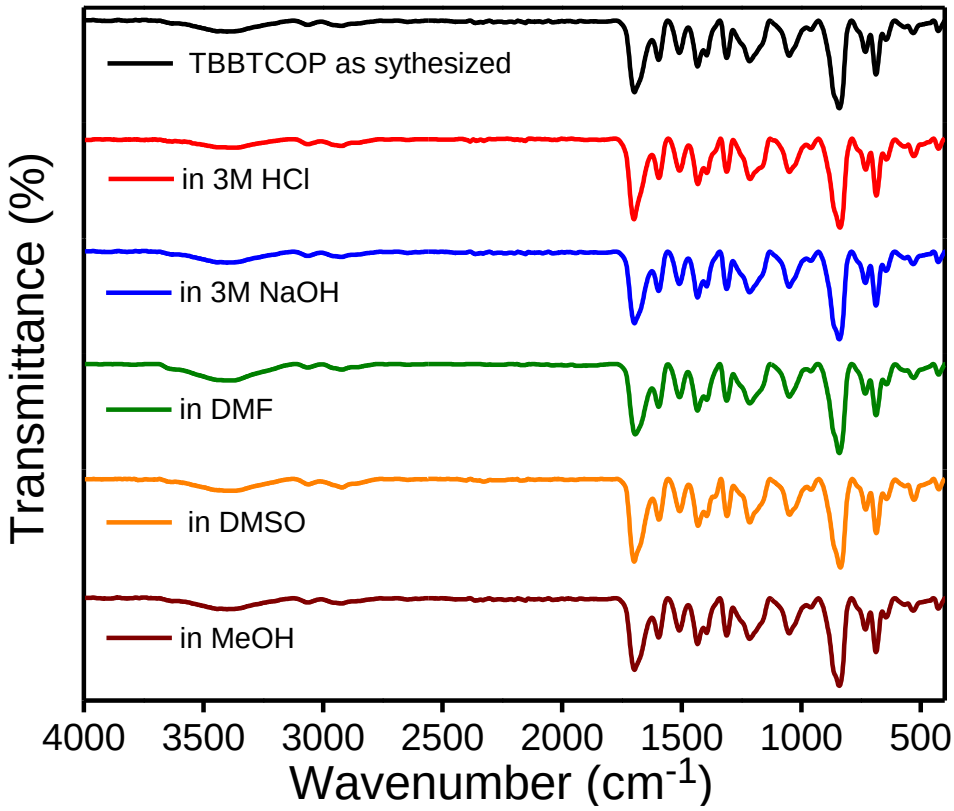

Figure 22. Stability test of TBBTCOP in different solvents.

In order to check the stability of our synthesized TBBTCOP, we performed the stability test in 3 M HCl, 3 M NaOH, DMF, DMSO and in MeOH. In all the cases, the COP retained its structure and no such change was observed in the FT-IR spectra showing its ultra stable nature.

5.8 Synthesis of Cu@TBBTCOP.

Since our synthesized TBBTCOP did not have active donor sites for coordinating to copper, hence we tried to grow Cu nanoparticles on our COP skeleton. So, $NaBH_4$ and ascorbic acid were the two different reducing agents that we tried for the synthesis. Among these we obtained better result for the C-N coupling when we used ascorbic acid as the reducing agent. Although currently, we do not have a viable explanation for such an observation however, further characterization of the copper incorporated TBBTCOP might shed some light on this topic.

5.9 Utilization of TBBTCOP in catalysis.

We tried to utilize TBBTCOP for C-C homo-coupling reaction involving 2,6-dimethoxyphenol. However, since our plan was to generate the active catalyst inside the reaction mixture using H_2O_2 and Ac_2O, majorly 2,6-dimethoxyphenol was converted to 2,6-dimethoxybenzoquinone and the corresponding acetate ester of 2,6-dimethoxyphenol.

Table 3. Optimization table for the metal free C-C homocoupling reaction.

Sr. No.	2,6-dimethoxy phenol	Hydrogen peroxide	Acetic anhydride	Solvent	TBBTCOP
1[a].	1 equiv.	1.25 equiv.	1.25 equiv.	DCM, AcOH	10 mg
2.	1 equiv.	8.0 equiv.	8.0 equiv.	DCM, AcOH	10 mg
3.	1 equiv.	8.0 equiv.	8.0 equiv.	Toluene, AcOH	10 mg
4.	1 equiv.	8.0 equiv.	8.0 equiv.	Toluene, AcOH	20 mg
5[b].	1 equiv.	8.0 equiv.	8.0 equiv.	Toluene, AcOH	20 mg

a. Active catalyst was generated *in situ*; b. active catalyst was generated separately.

Hence we shifted our focus on to a different reaction involving an arylboronic acid and an arylamine i.e. Chan-Lam coupling reaction. After incorporation of copper, Cu@TBBTCOP was tested for the C-N coupling reaction between phenylboronic acid and aniline using MeOH and H_2O

(2:1) as the solvent in which we obtained 73% conversion to diphenylamine after 60 h. However, when we tried to use *o*-toluidine and *m*-toluidine, we obtained small amounts of azo product along with our desired C-N coupled product. This led to a decreased yield of about 55% (isolated yield) in case of *m*-toluidine.

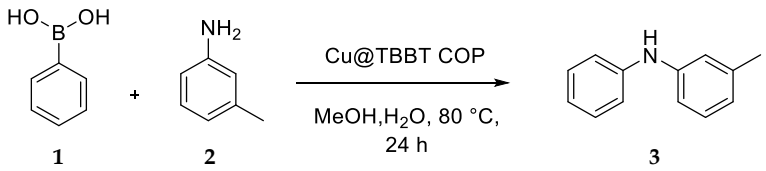

Scheme 13. C-N coupling reaction between phenylboronic acid and *m*-toluidine.

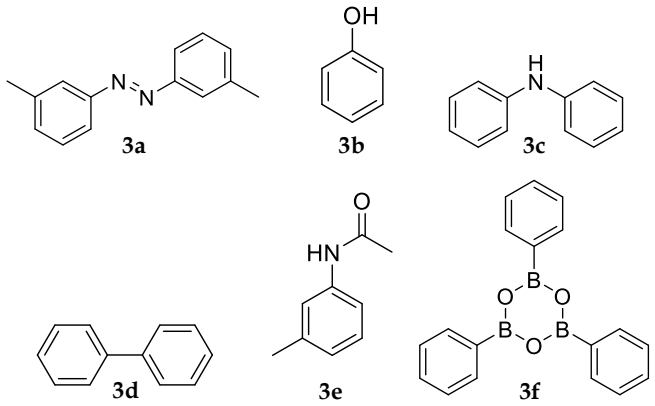

Figure 23. Probable products obtained during Chan-Lam coupling reaction between phenylboronic acid and *m*-toluidine.

Among all the possible products, **3a** and **3b** was observed in almost all scenarios along with our desired product **3**. However, products **3c** and **3d** were observed (in GCMS) when harsh conditions were used for the synthesis. Now, the origin of **3e** might be due to some unwanted side reaction between our aryl amine and acetate molecules which might trapped into our COP skeleton during the incorporation of copper as we have used copper acetate salt. Also **3f** was observed when dry solvents were used for this conversion.

Table 4. Optimization table for Chan-Lam coupling reaction between phenylboronic acid and *m*-toluidine.

Sr. No.	**1**	**2**	Cu@TBBTCOP	Solvent	% Conversion[c]						
					3	**3a**	**3b**	**3c**	**3d**	**3e**	**3f**
1.	1.25 equiv.	1.0 equiv.	10 mg	MeOH, H_2O	**23**	**12**	**10**	**8**	**0**	**9**	**0**
2.	1.25 equiv.	1.0 equiv.	15 mg	MeOH, H_2O	**22**	**9**	**8**	**10**	**0**	**10**	**0**
3[a].	1.5 equiv.	1.0 equiv.	20 mg	MeOH, H_2O	**24**	**18**	**8**	**7**	**7**	**5**	**0**
4.	1.5 equiv.	1.0 equiv.	10 mg	MeOH, H_2O	**38**	**19**	**10**	**7**	**0**	**0**	**0**
5[b].	2.0 equiv.	1.0 equiv.	10 mg	MeOH, H_2O	**9**	**3**	**4**	**0**	**0**	**0**	**0**
6.	2.0 equiv.	1.0 equiv.	10 mg	THF	**15**	**9**	**5**	**8**	**3**	**7**	**12**
7.	2.0 equiv.	1.0 equiv.	10 mg	1,4-dioxane	**20**	**7**	**7**	**7**	**4**	**8**	**15**

a. Reaction was performed under microwave radiation; b. NEt_3 was added; c. GCMS yield

Chapter 6

CONCLUSION AND FUTURE SCOPE

We have successfully synthesized TPTC and characterized it with the help of ^{1}H and ^{13}C NMR. TBBTCOP was synthesized via microwave assisted synthesis in just 3 h and was characterized using FT-IR, PXRD, FE-SEM, TGA and BET analysis. TBBTCOP shows low crystallinity with high stability under acidic as well as basic conditions.

Copper was successfully incorporated inside our material and was used for the Chan-Lam C-N coupling reaction. The reaction between phenylboronic acid and aniline resulted in the formation of diphenylamine with an isolated yield of about 73%. However, when aniline was replaced by *m*-toluidine, the yield decreased to about 55% due to formation of other side products. Hence more optimization is required so that we can obtain our desired product via C-N coupling in good yields.

Further characterization of the Cu@TBBTCOP is required in order to predict the mechanism for the C-N coupling reaction. We also need to look for the extent of Cu loading in our COP. Upon further optimization, this Cu@TBBTCOP could be used for C-N coupling reaction for a wide variety of substrates.

Apart from the Chan-Lam coupling reaction, we are now trying to use the TBBTCOP for gas sensing purposes. After a few number of tries, TBBTCOP has shown specific selectivity for ammonia gas **(Figure 22)** and we will be further exploring this in order to get a complete idea about the use of our TBBTCOP for practical gas sensing applications.

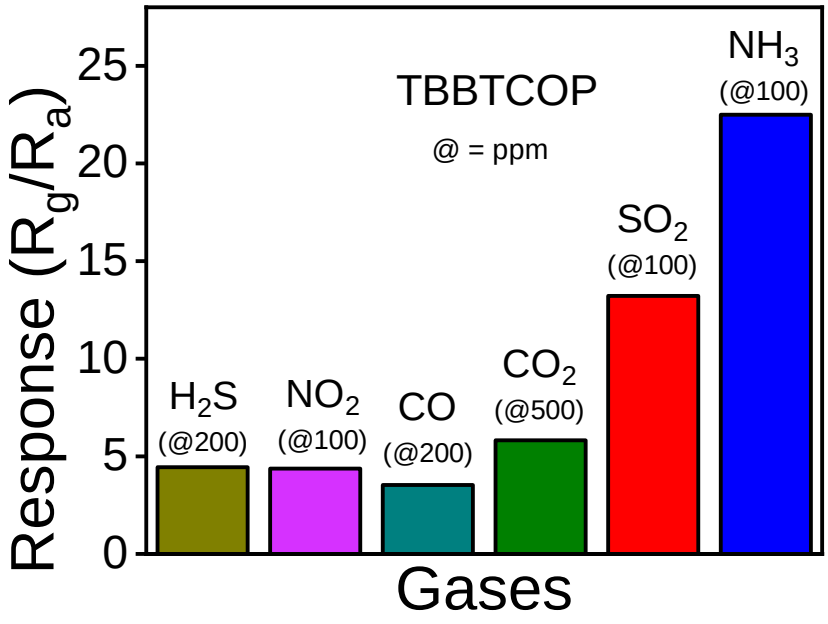

Figure 24. Selectivity of TBBTCOP sensor against different gases.

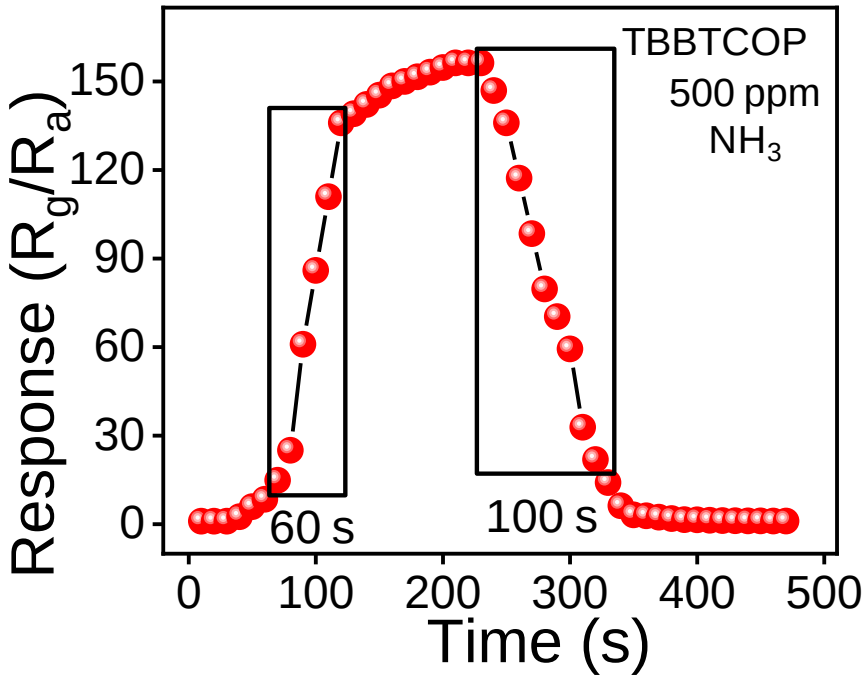

Figure 25. Single transient response–recovery cycle of TBBTCOP toward 500 ppm of NH_3.

REFERENCES

[1] Côté, A. P.; Benin, A. I.; Ockwig, N. W.; O'Keeffe, M.; Matzger, A. J.; Yaghi, O. M. Porous, Crystalline, Covalent Organic Frameworks. *Science* **2005**, *310*, 1166-1170, DOI: 10.1126/science.1120411.

[2] Waller, P. J.; Gándara, F.; Yaghi, O. M. Chemistry of Covalent Organic Frameworks. *Acc. Chem. Res.* **2015**, *48*, 3053–3063, DOI:10.1021/acs.accounts.5b00369.

[3] Das, G.; Balaji Shinde, D.; Kandambeth, S.; Biswal, B. P.; Banerjee, R. Mechanosynthesis of Imine, β-Ketoenamine, and Hydrogen-Bonded Imine-Linked Covalent Organic Frameworks Using Liquid-Assisted Grinding. *Chem. Commun.* **2014**, *50*, 12615–12618, DOI: 10.1039/C4CC03389B.

[4] Lanni, L. M.; Tilford, R. W.; Bharathy, M.; Lavigne, J. J. Enhanced Hydrolytic Stability of Self-Assembling Alkylated Two-Dimensional Covalent Organic Frameworks. *J. Am. Chem. Soc.* **2011**, *133*, 13975–13983, DOI: 10.1021/ja203807h.

[5] Uribe-Romo, F. J.; Hunt, J. R.; Furukawa, H.; Klöck, C.; O'Keeffe, M.; Yaghi, O. M. A Crystalline Imine-Linked 3-D Porous Covalent Organic Framework. *J. Am. Chem. Soc.* **2009**, *131*, 4570–4571, DOI: 10.1021/ja8096256.

[6] Stegbauer, L.; Schwinghammer, K.; Lotsch, B. V. A Hydrazone-Based Covalent Organic Framework for Photocatalytic Hydrogen Production. *Chem. Sci.* **2014**, *5*, 2789–2793, DOI: 10.1039/C4SC00016A.

[7] Guo, J.; Xu, Y.; Jin, S.; Chen, L.; Kaji, T.; Honsho, Y.; Addicoat, M. A.; Kim, J.; Saeki, A.; Ihee, H.; Seki, S.; Irle, S.; Hiramoto, M.; Gao, J.; Jiang, D. Conjugated Organic Framework with Three-Dimensionally Ordered Stable Structure

and Delocalized π Clouds. *Nat. Commun.* **2013**, *4*, 2736, DOI: 10.1038/ncomms3736.

[8] Xu, T.; Li, Y.; Zhao, Z.; Xing, G.; Chen, L. *N* , *N* ′-Bicarbazole-Based Covalent Triazine Frameworks as High-Performance Heterogeneous Photocatalysts. *Macromolecules* **2019**, *52*, 9786–9791, DOI: 10.1021/acs.macromol.9b01771.

[9] Wang, X.; Zhang, S.; Li, X.; Zhan, Z.; Tan, B.; Lang, X.; Jin, S. Two-Dimensional Crystalline Covalent Triazine Frameworks *via* Dual Modulator Control for Efficient Photocatalytic Oxidation of Sulfides. *J. Mater. Chem. A* **2021**, *9*, 16405–16410, DOI: 10.1039/D1TA03951B.

[10] Luan, T.-X.; Du, L.; Wang, J.-R.; Li, K.; Zhang, Q.; Li, P.-Z.; Zhao, Y. Highly Effective Generation of Singlet Oxygen by an Imidazole-Linked Robust Photosensitizing Covalent Organic Framework. *ACS Nano* **2022**, *16*, 21565–21575, DOI: 10.1021/acsnano.2c10423.

[11] Rowan, S. J.; Cantrill, S. J.; Cousins, G. R. L.; Sanders, J. K. M.; Stoddart, J. F. Dynamic Covalent Chemistry. *Angew. Chem. Int. Ed.* **2002**, *41*, 898–952, DOI: 10.1002/1521-3773(20020315)41:6<898::AID-ANIE898>3.0.CO;2-E.

[12] Jin, Y.; Yu, C.; Denman, R. J.; Zhang, W. Recent Advances in Dynamic Covalent Chemistry. *Chem. Soc. Rev.* **2013**, *42*, 6634, DOI: 10.1039/c3cs60044k.

[13] Geng, K.; He, T.; Liu, R.; Dalapati, S.; Tan, K. T.; Li, Z.; Tao, S.; Gong, Y.; Jiang, Q.; Jiang, D. Covalent Organic Frameworks: Design, Synthesis, and Functions. *Chem. Rev.* **2020**, *120*, 8814–8933, DOI: 10.1021/acs.chemrev.9b00550.

[14] Kandambeth, S.; Dey, K.; Banerjee, R. Covalent Organic Frameworks: Chemistry beyond the Structure. *J. Am. Chem. Soc.* **2019**, *141*, 1807–1822, DOI: 10.1021/jacs.8b10334.

[15] Kandambeth, S.; Mallick, A.; Lukose, B.; Mane, M. V.; Heine, T.; Banerjee, R. Construction of Crystalline 2D Covalent Organic Frameworks with Remarkable Chemical (Acid/Base) Stability via a Combined Reversible and Irreversible Route. *J. Am. Chem. Soc.* **2012**, *134*, 19524–19527, DOI: 10.1021/ja308278w.

[16] Wei, P.-F.; Qi, M.-Z.; Wang, Z.-P.; Ding, S.-Y.; Yu, W.; Liu, Q.; Wang, L.-K.; Wang, H.-Z.; An, W.-K.; Wang, W. Benzoxazole-Linked Ultrastable Covalent Organic Frameworks for Photocatalysis. *J. Am. Chem. Soc.* **2018**, *140*, 4623–4631, DOI: 10.1021/jacs.8b00571.

[17] Waller, P. J.; AlFaraj, Y. S.; Diercks, C. S.; Jarenwattananon, N. N.; Yaghi, O. M. Conversion of Imine to Oxazole and Thiazole Linkages in Covalent Organic Frameworks. *J. Am. Chem. Soc.* **2018**, *140*, 9099–9103, DOI: 10.1021/jacs.8b05830.

[18] Haase, F.; Troschke, E.; Savasci, G.; Banerjee, T.; Duppel, V.; Dörfler, S.; Grundei, M. M. J.; Burow, A. M.; Ochsenfeld, C.; Kaskel, S.; Lotsch, B. V. Topochemical Conversion of an Imine- into a Thiazole-Linked Covalent Organic Framework Enabling Real Structure Analysis. *Nat. Commun.* **2018**, *9*, 2600, DOI: 10.1038/s41467-018-04979-y.

[19] Vyas, V. S.; Vishwakarma, M.; Moudrakovski, I.; Haase, F.; Savasci, G.; Ochsenfeld, C.; Spatz, J. P.; Lotsch, B. V. Exploiting Noncovalent Interactions in an Imine-Based Covalent Organic Framework for Quercetin Delivery. *Adv. Mater.* **2016**, *28*, 8749–8754, DOI: 10.1002/adma.201603006.

[20] Paul, R.; Chandra Shit, S.; Mandal, H.; Rabeah, J.; Kashyap, S. S.; Nailwal, Y.; Shinde, D. B.; Lai, Z.; Mondal, J. Benzothiazole-Linked Metal-Free Covalent Organic Framework Nanostructures for Visible-Light-Driven Photocatalytic Conversion of Phenylboronic Acids to Phenols. *ACS Appl. Nano Mater.* **2021**, *4*, 11732–11742, DOI: 10.1021/acsanm.1c02329.

[21] Cusin, L.; Peng, H.; Ciesielski, A.; Samorì, P. Chemical Conversion and Locking of the Imine Linkage: Enhancing the Functionality of Covalent Organic Frameworks. *Angew. Chem. Int. Ed.* **2021**, *133*, 14356–14370, DOI: 10.1002/ange.202016667.

[22] Wang, K.; Jia, Z.; Bai, Y.; Wang, X.; Hodgkiss, S. E.; Chen, L.; Chong, S. Y.; Wang, X.; Yang, H.; Xu, Y.; Feng, F.; Ward, J. W.; Cooper, A. I. Synthesis of Stable Thiazole-Linked Covalent Organic Frameworks via a Multicomponent Reaction. *J. Am. Chem. Soc.* **2020**, *142*, 11131–11138, DOI: 10.1021/jacs.0c03418.

[23] Li, X.; Cai, S.; Sun, B.; Yang, C.; Zhang, J.; Liu, Y. Chemically Robust Covalent Organic Frameworks: Progress and Perspective. *Matter* **2020**, *3*, 1507–1540, DOI: 10.1016/j.matt.2020.09.007.

[24] Li, T.; Yan, X.; Liu, Y.; Zhang, W.-D.; Fu, Q.-T.; Zhu, H.; Li, Z.; Gu, Z.-G. A 2D Covalent Organic Framework Involving Strong Intramolecular Hydrogen Bonds for Advanced Supercapacitors. *Polym. Chem.* **2020**, *11*, 47–52, DOI: 10.1039/C9PY01623F.